Security-aware Semantic-driven ISAC via Paired Adversarial Residual Networks

Yu Liu, Boxiang He, and Fanggang Wang, *Senior Member*, *IEEE*

***Abstract*—This paper proposes a novel and flexible security-aware semantic-driven integrated sensing and communication (ISAC) framework, namely security semantic ISAC (SS-ISAC). Inspired by the positive impact of the adversarial attack, a pair of pluggable encryption and decryption modules is designed in the proposed SS-ISAC framework. The encryption module is installed after the semantic transmitter, adopting a trainable adversarial residual network (ARN) to create the adversarial attack. Correspondingly, the decryption module before the semantic receiver utilizes another trainable ARN to mitigate the adversarial attack and noise. These two modules can be flexibly assembled considering the system security demands, without drastically modifying the hardware infrastructure. To ensure the sensing and communication (SAC) performance while preventing the eavesdropping threat, the above ARNs are jointly optimized by minimizing a carefully designed loss function that relates to the adversarial attack power, SAC performance, as well as the privacy leakage risk. Simulation results validate the effectiveness of the proposed SS-ISAC framework in terms of both SAC and eavesdropping prevention performance.**

***Index Terms*—Adversarial attack, integrated sensing and communication (ISAC), semantic transceiver, wireless security.**

I. Introduction

THE integrated sensing and communication (ISAC) has emerged as a promising paradigm to revolutionize the landscape of future wireless system generations, such as the ISAC-enabler railway, vehicular, and unmanned aerial vehicles systems, meeting their enhanced spectral/energy efficiency demands [1]–[3]. The performance tradeoff between sensing and communication (SAC) functionalities is a crucial research topic in the ISAC-enabler systems. The sensing-assisted communication aims to optimize the communication efficiency/reliability under the constraints of acceptable sensing metrics [4], [5], whereas the communication-assisted sensing sheds light on optimizing the sensing functionalities (e.g., vehicle location/speed estimation accuracy) [6].

Semantic communication is another revolutionary paradigm for future wireless system generations, aiming to transmit the underlying meaning of source messages rather than their exact bits [7]. The integration of the semantic communication concept with ISAC systems has revealed profound potential in addressing resource scarcity. Motivated by the advancement of deep neural network (DNN), various DNN models have been adopted to facilitate the semantic-driven ISAC system design, achieving promising SAC performance improvement [8]. However, along with the above benefits, the vulnerability of the DNN models and broadcast nature of the wireless channels also make semantic-driven ISAC systems more susceptible to eavesdropping threats. Recently, the security problems in the semantic-driven ISAC systems have drawn research attention. For instance, the authors in [9] maximized the secure semantic efficiency, and [10] optimized the transmit beamforming matrix and semantic extraction ratio under the constraints of the acceptable SAC performance. Although the existing literature has made crucial contributions to counter eavesdropping, it is required to redesign/retrain the overall semantic-driven ISAC system when facing security demands, leading to an unacceptable extra computational cost.

To fulfill the above research gap, this paper proposes a novel and flexible security-aware semantic-driven ISAC framework, referred to as security semantic ISAC (SS-ISAC). The main contributions are outlined as follows:

1) A SS-ISAC framework is developed, involving a pair of pluggable encryption and decryption modules. The encryption module located after the semantic transmitter is utilized to generate the adversarial attack and counter eavesdropping, while the decryption module before the semantic receiver mitigates the adversarial attack and noise. The above modules can be flexibly assembled according to the security demands, without drastically modifying the entire system.
2) The encryption and decryption modules are realized by the paired adversarial residual networks (ARNs). Moreover, the paired ARNs are jointly optimized by minimizing a precisely designed loss function that comprehensively considers the adversarial attack power limit, SAC performance, and privacy leakage risk.
3) Numerical results demonstrate the promising performance achieved by the proposed SS-ISAC framework, including high system compatibility, satisfactory SAC performance, and low privacy leakage risk.

II. General Semantic-Driven ISAC System

Consider a general semantic-driven ISAC system with a full-duplex ISAC base station (BS), target, and downlink user equipment (UE), as illustrated in Fig. 1. This system is named as the general semantic ISAC (GS-ISAC). The ISAC BS is equipped with M transmit antennas and one receive antenna to sense the target, while communicating with the single-antenna downlink UE. As shown in the upper part of Fig. 2, the semantic transmitter at the ISAC BS consists of a semantic encoder (SE) and joint source channel encoder (JSCE), whereas the semantic receivers at the ISAC BS and downlink UE are respectively composed of a semantic decoder (SD) and joint source channel decoder (JSCD). On this basis,

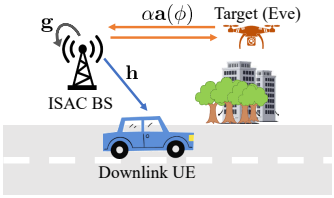

Fig. 1. GS-ISAC system model.

the SE network $\mathcal{E}^{\mathrm{SE}}(\cdot)$ extracts the semantic information, $\mathbf{x}'$, as

$$\mathbf{x}' = \mathcal{E}^{\mathrm{SE}}(\mathbf{x}; \boldsymbol{\theta}^{\mathrm{SE}}), \tag{1}$$

where $\mathbf{x} \in \mathbb{R}^{1\times L_{\mathrm{x}}}$ represents the source data with the length of L_{x}, and $\boldsymbol{\theta}^{\mathrm{SE}}(\cdot)$ denotes the network parameters of $\mathcal{E}^{\mathrm{SE}}(\cdot)$. By feeding $\mathbf{x}'$ into the JSCE network $\mathcal{E}^{\mathrm{JSCE}}(\cdot)$, the transmitted signal at the ISAC BS, $\mathbf{z} \in \mathbb{R}^{1\times L_{\mathrm{z}}}$, is generated as

$$\mathbf{z} = \mathcal{E}^{\mathrm{JSCE}}(\mathbf{x}'; \boldsymbol{\theta}^{\mathrm{JSCE}}), \tag{2}$$

where $\boldsymbol{\theta}^{\mathrm{JSCE}}$ is the network parameters of $\mathcal{E}^{\mathrm{JSCE}}(\cdot)$ and $L_{\mathrm{z}} < L_{\mathrm{x}}$. Here, $\mathcal{E}^{\mathrm{SE}}(\cdot)$ aims to extract the task-relevant feature, while $\mathcal{E}^{\mathrm{JSCE}}(\cdot)$ is used to compress the semantic information and combat the interference during wireless transmission.

Then, the received SAC signals, $\mathbf{y}_{\mathrm{BS}}$ and $\mathbf{y}_{\mathrm{UE}}$, at the ISAC BS and downlink UE are respectively given by

$$\mathbf{y}_{\mathrm{BS}} = \underbrace{\alpha\mathbf{a}^{\mathrm{H}}(\phi)\mathbf{w}\mathbf{z}}_{\text{Sensing signal}} + \underbrace{\mathbf{g}^{\mathrm{H}}\mathbf{z}}_{\text{Residual SI}} + \mathbf{n}_{\mathrm{BS}}, \tag{3}$$

and

$$\mathbf{y}_{\mathrm{UE}} = \underbrace{\mathbf{h}^{\mathrm{H}}\mathbf{w}\mathbf{z}}_{\text{Communication Signal}} + \mathbf{n}_{\mathrm{UE}}, \tag{4}$$

where $\alpha\mathbf{a}(\phi) \in \mathbb{C}^{M\times 1}$, $\mathbf{g} \in \mathbb{C}^{M\times 1}$, and $\mathbf{h} \in \mathbb{C}^{M\times 1}$ respectively denote the channels of sensing, self-interference (SI), and communication, while $\mathbf{w} \in \mathbb{C}^{M\times 1}$ is the transmit beamforming vector. Here, α is the complex-valued reflection coefficient of the target. The steering vector $\mathbf{a}(\phi)$ associated with the target azimuth angle ϕ is defined as $\mathbf{a}(\phi) = [1, e^{\jmath\frac{2\pi d}{\lambda}\sin(\phi)}, \ldots, e^{\jmath\frac{2\pi d}{\lambda}(M-1)\sin(\phi)}]^{\mathrm{T}}$, with d and λ as the transmit antenna spacing of ISAC BS and the signal wavelength, respectively [2]. Due to the full-duplex operation mode, the SI is induced to the ISAC BS receiver through the SI channel $\mathbf{g} \in \mathbb{C}^{M\times 1}$. Before target sensing, $\mathbf{g}$ can be pre-estimated, and the residual SI term in (3) is compensated, considering a slow-varying propagation environment between the ISAC BS transceiver [11]. Moreover, before accomplishing the communication task, the channel information $\mathbf{h}' = \mathbf{h}^{\mathrm{H}}\mathbf{w}$ in (4) has been accessed since the downlink UE can receive a pilot signal to pre-estimate $\mathbf{h}'$ [3]. The noise $\mathbf{n}_{\mathrm{BS}}$ and $\mathbf{n}_{\mathrm{UE}}$ respectively follow the zero-mean Gaussian distribution $\mathcal{CN}(0, \sigma_{\mathrm{BS}}^2\mathbf{I}_{L_{\mathrm{z}}})$ with variance of σ_{BS}^2 and $\mathcal{CN}(0, \sigma_{\mathrm{UE}}^2\mathbf{I}_{L_{\mathrm{z}}})$ with variance of σ_{UE}^2. Furthermore, by utilizing the JSCD networks $\mathcal{D}_{\mathrm{BS}}^{\mathrm{JSCD}}(\cdot)$ and $\mathcal{D}_{\mathrm{UE}}^{\mathrm{JSCD}}(\cdot)$, the recovered semantic information at the ISAC BS and downlink UE, $\hat{\mathbf{x}}'_{\mathrm{BS}}$ and $\hat{\mathbf{x}}'_{\mathrm{UE}}$, are respectively written as

$$\hat{\mathbf{x}}'_{\mathrm{BS}} = \mathcal{D}_{\mathrm{BS}}^{\mathrm{JSCD}}\left(\mathbf{y}_{\mathrm{BS}}; \boldsymbol{\theta}_{\mathrm{BS}}^{\mathrm{JSCD}}\right), \tag{5}$$

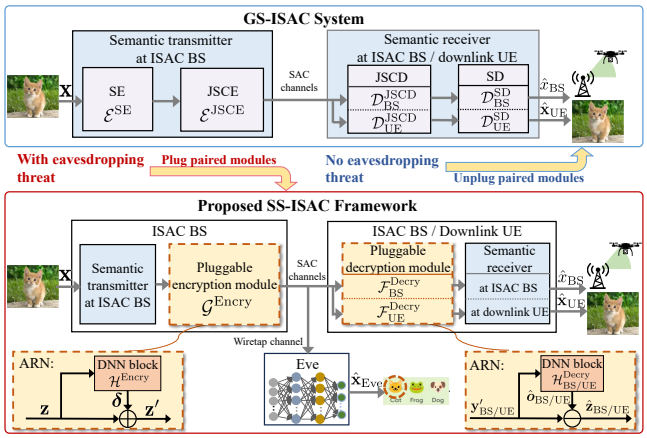

Fig. 2. Signal transmitting and receiving process in the GS-ISAC system and proposed SS-ISAC framework.

and

$$\hat{\mathbf{x}}'_{\mathrm{UE}} = \mathcal{D}_{\mathrm{UE}}^{\mathrm{JSCD}}\left(\mathbf{y}_{\mathrm{UE}}; \boldsymbol{\theta}_{\mathrm{UE}}^{\mathrm{JSCD}}\right), \tag{6}$$

where $\boldsymbol{\theta}_{\mathrm{BS}}^{\mathrm{JSCD}}$ and $\boldsymbol{\theta}_{\mathrm{UE}}^{\mathrm{JSCD}}$ denote the network parameters of $\mathcal{D}_{\mathrm{BS}}^{\mathrm{JSCD}}(\cdot)$ and $\mathcal{D}_{\mathrm{UE}}^{\mathrm{JSCD}}(\cdot)$, respectively. The primary function of the JSCD is to recover the transmitted semantic features and mitigate the channel interference. Then, the SD networks at the ISAC BS and downlink UE, $\mathcal{D}_{\mathrm{BS}}^{\mathrm{SD}}(\cdot)$ and $\mathcal{D}_{\mathrm{UE}}^{\mathrm{SD}}(\cdot)$, respectively output the final results of the SAC tasks as

$$\hat{x}_{\mathrm{BS}} = \mathcal{D}_{\mathrm{BS}}^{\mathrm{SD}}\left(\hat{\mathbf{x}}'_{\mathrm{BS}}; \boldsymbol{\theta}_{\mathrm{BS}}^{\mathrm{SD}}\right), \tag{7}$$

and

$$\hat{\mathbf{x}}_{\mathrm{UE}} = \mathcal{D}_{\mathrm{UE}}^{\mathrm{SD}}\left(\hat{\mathbf{x}}'_{\mathrm{UE}}; \boldsymbol{\theta}_{\mathrm{UE}}^{\mathrm{SD}}\right), \tag{8}$$

where $\boldsymbol{\theta}_{\mathrm{BS}}^{\mathrm{SD}}$ and $\boldsymbol{\theta}_{\mathrm{UE}}^{\mathrm{SD}}$ are the network parameters of $\mathcal{D}_{\mathrm{BS}}^{\mathrm{SD}}(\cdot)$ and $\mathcal{D}_{\mathrm{UE}}^{\mathrm{SD}}(\cdot)$, respectively.

Taking the target azimuth estimation and image transmission as examples to investigate the GS-ISAC system. In this case, $\hat{x}_{\mathrm{BS}}$ represents the target azimuth estimation result for the sensing task, while $\hat{\mathbf{x}}_{\mathrm{UE}}$ is the recovered source data for the communication task. The loss function $\mathcal{L}(\boldsymbol{\Theta}_{\mathrm{General}})$ is adopted to jointly train the networks in the GS-ISAC system as

$$\mathcal{L}(\boldsymbol{\Theta}_{\mathrm{General}}) = \gamma_{\mathrm{sen}}\mathcal{L}_{\mathrm{sen}} + \gamma_{\mathrm{com}}\mathcal{L}_{\mathrm{com}}, \tag{9}$$

where $\boldsymbol{\Theta}_{\mathrm{General}} = \{\boldsymbol{\theta}^{\mathrm{SE}}, \boldsymbol{\theta}^{\mathrm{JSCE}}, \boldsymbol{\theta}_{\mathrm{BS}}^{\mathrm{JSCD}}, \boldsymbol{\theta}_{\mathrm{BS}}^{\mathrm{SD}}, \boldsymbol{\theta}_{\mathrm{UE}}^{\mathrm{JSCD}}, \boldsymbol{\theta}_{\mathrm{UE}}^{\mathrm{SD}}\}$ denotes the network parameters set. The hyperparameters γ_{sen} and γ_{com} are used to pursue the tradeoff between SAC performance. The loss functions $\mathcal{L}_{\mathrm{sen}}$ and $\mathcal{L}_{\mathrm{com}}$, respectively describing the SAC performance, are further illustrated in Section III-B. Once the trained parameters set $\hat{\boldsymbol{\Theta}}_{\mathrm{General}}$ is obtained, the GS-ISAC system can employ the trained SE, JSCE, JSCD, and SD networks in the practical SAC tasks.

III. Proposed SS-ISAC Framework Design

This section considers the eavesdropping threat faced in the semantic-driven ISAC system. To deal with this threat, a novel SS-ISAC framework is firstly proposed, which assembles a pair of pluggable modules to the original GS-ISAC system. Then, the paired pluggable modules are carefully designed based on the ARNs.

A. SS-ISAC Framework via Paired Pluggable Modules

Consider a SS-ISAC framework, as illustrated in the bottom part of Fig. 2. The ISAC BS and downlink UE respectively focus on the legitimate SAC tasks, whereas the target is a potential eavesdropper (i.e., namely Eve) and attempts to eavesdrop on the privacy information from the ISAC BS. To ensure the system security, a pluggable encryption module is installed after the semantic transmitter of the ISAC BS. In this case, the transmitted signal at the ISAC BS, $\mathbf{z}'$, is written as

$$\mathbf{z}' = \mathcal{G}^{\mathrm{Encry}}(\mathbf{z}; \boldsymbol{\theta}^{\mathrm{Encry}}), \tag{10}$$

where $\mathcal{G}^{\mathrm{Encry}}(\cdot)$ is the pluggable encryption module to be devised, and $\boldsymbol{\theta}^{\mathrm{Encry}}$ denotes its network parameters. Then, the received SAC signals at the ISAC BS and downlink UE, $\mathbf{y}'_{\mathrm{BS}}$ and $\mathbf{y}'_{\mathrm{UE}}$, are respectively expressed as

$$\mathbf{y}'_{\mathrm{BS}} = \underbrace{\alpha \mathbf{a}^{\mathrm{H}}(\phi)\mathbf{w}\mathbf{z}'}_{\text{Sensing signal}} + \underbrace{\mathbf{g}^{\mathrm{H}}\mathbf{z}'}_{\text{Residual SI}} + \mathbf{n}_{\mathrm{BS}}, \tag{11}$$

and

$$\mathbf{y}'_{\mathrm{UE}} = \underbrace{\mathbf{h}^{\mathrm{H}}\mathbf{w}\mathbf{z}'}_{\text{Communication signal}} + \mathbf{n}_{\mathrm{UE}}. \tag{12}$$

The received signal at Eve, $\mathbf{y}'_{\mathrm{Eve}}$, is given by

$$\mathbf{y}'_{\mathrm{Eve}} = \underbrace{\alpha \mathbf{a}^{\mathrm{H}}(\phi)\mathbf{w}\mathbf{z}'}_{\text{Eavesdropping signal}} + \mathbf{n}_{\mathrm{Eve}}, \tag{13}$$

where $\mathbf{n}_{\mathrm{Eve}}$ is the noise that follows $\mathcal{CN}(0, \sigma^2_{\mathrm{Eve}}\mathbf{I}_{L_z})$ with zero-mean and variance of σ^2_{Eve}. For the legitimate ISAC BS and downlink UE, the pluggable decryption modules are respectively added in front of their semantic receiver. As such, the outputs of the pluggable decryption modules, $\hat{\mathbf{z}}_{\mathrm{BS}}$ and $\hat{\mathbf{z}}_{\mathrm{UE}}$, are respectively written as

$$\hat{\mathbf{z}}_{\mathrm{BS}} = \mathcal{F}^{\mathrm{Decry}}_{\mathrm{BS}}\big(\mathbf{y}'_{\mathrm{BS}}; \boldsymbol{\theta}^{\mathrm{Decry}}_{\mathrm{BS}}\big), \tag{14}$$

and

$$\hat{\mathbf{z}}_{\mathrm{UE}} = \mathcal{F}^{\mathrm{Decry}}_{\mathrm{UE}}\big(\mathbf{y}'_{\mathrm{UE}}; \boldsymbol{\theta}^{\mathrm{Decry}}_{\mathrm{UE}}\big), \tag{15}$$

where $\mathcal{F}^{\mathrm{Decry}}_{\mathrm{BS}}(\cdot)$ and $\mathcal{F}^{\mathrm{Decry}}_{\mathrm{UE}}(\cdot)$ are respectively the pluggable decryption modules to be designed at the ISAC BS and downlink UE. Their corresponding network parameters are $\boldsymbol{\theta}^{\mathrm{Decry}}_{\mathrm{BS}}$ and $\boldsymbol{\theta}^{\mathrm{Decry}}_{\mathrm{UE}}$, respectively. Finally, the ISAC BS outputs the estimation result of the target azimuth angle as

$$\hat{x}_{\mathrm{BS}} = \mathcal{D}^{\mathrm{SD}}_{\mathrm{BS}}\Big(\mathcal{D}^{\mathrm{JSCD}}_{\mathrm{BS}}\big(\hat{\mathbf{z}}_{\mathrm{BS}}; \boldsymbol{\theta}^{\mathrm{JSCD}}_{\mathrm{BS}}\big); \boldsymbol{\theta}^{\mathrm{SD}}_{\mathrm{BS}}\Big), \tag{16}$$

and the downlink UE recovers the source data as

$$\hat{\mathbf{x}}_{\mathrm{UE}} = \mathcal{D}^{\mathrm{SD}}_{\mathrm{UE}}\Big(\mathcal{D}^{\mathrm{JSCD}}_{\mathrm{UE}}\big(\hat{\mathbf{z}}_{\mathrm{UE}}; \boldsymbol{\theta}^{\mathrm{JSCD}}_{\mathrm{UE}}\big); \boldsymbol{\theta}^{\mathrm{SD}}_{\mathrm{UE}}\Big). \tag{17}$$

For the eavesdropper Eve, the privacy information, $\hat{\mathbf{x}}_{\mathrm{Eve}}$, is inferred by using its own DNN $\mathcal{P}_{\mathrm{Eve}}(\cdot)$ as

$$\hat{\mathbf{x}}_{\mathrm{Eve}} = \mathcal{P}_{\mathrm{Eve}}(\mathbf{y}'_{\mathrm{Eve}}; \boldsymbol{\theta}_{\mathrm{Eve}}). \tag{18}$$

The above proposed SS-ISAC framework aims to carefully design the paired pluggable encryption and decryption modules (i.e., $\mathcal{G}^{\mathrm{Encry}}$ and $\mathcal{F}^{\mathrm{Decry}}_{\mathrm{BS/UE}}$), so as to guarantee the security of the SAC tasks, without re-training the original semantic transceivers. Specifically, it should ensure that the ISAC BS can estimate the target azimuth angle accurately, and the downlink UE recovers reliable source data of the image, whereas Eve infers the privacy information (i.e., image label) with a high error probability.

B. ARN-based Paired Pluggable Modules Design

Here, the specific design for the paired pluggable modules is presented. In the field of adversarial machine learning, it has been proven that even adding a small adversarial attack perturbation, the performance of the DNN models can be significantly degraded [7]. Inspired by the above concept, the pluggable encryption module is devised based on the adversarial attack, so as to fool the eavesdropper Eve. Then, the pluggable encryption module $\mathcal{G}^{\mathrm{Encry}}(\cdot)$ at the ISAC BS generates the adversarial examples, $\mathbf{z}'$, as

$$\begin{aligned}\mathbf{z}' &= \mathcal{G}^{\mathrm{Encry}}(\mathbf{z}; \boldsymbol{\theta}^{\mathrm{Encry}}) \\ &= \underbrace{\mathbf{z} + \mathcal{H}^{\mathrm{Encry}}(\mathbf{z}; \bar{\boldsymbol{\theta}}^{\mathrm{Encry}})}_{\text{ARN at ISAC BS transmitter}} \qquad (19) \\ &= \mathbf{z} + \boldsymbol{\delta}, \qquad (20)\end{aligned}$$

where $\mathcal{H}^{\mathrm{Encry}}(\cdot)$ represents a DNN block, with the network parameters of $\bar{\boldsymbol{\theta}}^{\mathrm{Encry}}$. The generated adversarial attack $\boldsymbol{\delta}$ from the DNN block is with a low-power of $\mathbb{E}(\frac{1}{L_{\mathrm{t}}}\|\boldsymbol{\delta}\|^2) \leq \tau$. Here, τ denotes a small power limit, and L_{t} is the length of $\boldsymbol{\delta}$. Note that (19) essentially describes an ARN. The advantage of the designed ARN is that it can learn the residuals, rather than directly training a mapping between network inputs and outputs, thereby improving the stability and speed of the network training. In other words, learning $\boldsymbol{\delta}$ is much easier than directly regenerating the network output $\mathbf{z}'$ from the input $\mathbf{z}$. Accordingly, the pluggable decryption modules $\mathcal{F}^{\mathrm{Decry}}_{\mathrm{BS}}(\cdot)$ and $\mathcal{F}^{\mathrm{Decry}}_{\mathrm{UE}}(\cdot)$ respectively output the decryption examples, $\hat{\mathbf{z}}_{\mathrm{BS}}$ and $\hat{\mathbf{z}}_{\mathrm{UE}}$, as

$$\begin{aligned}\hat{\mathbf{z}}_{\mathrm{BS}} &= \mathcal{F}^{\mathrm{Decry}}_{\mathrm{BS}}(\mathbf{y}'_{\mathrm{BS}}; \boldsymbol{\theta}^{\mathrm{Decry}}_{\mathrm{BS}}) \\ &= \underbrace{\mathbf{y}'_{\mathrm{BS}} - \mathcal{H}^{\mathrm{Decry}}_{\mathrm{BS}}(\mathbf{y}'_{\mathrm{BS}}; \bar{\boldsymbol{\theta}}^{\mathrm{Decry}}_{\mathrm{BS}})}_{\text{ARN at ISAC BS receiver}} \qquad (21) \\ &= \mathbf{y}'_{\mathrm{BS}} - \hat{\boldsymbol{o}}_{\mathrm{BS}}, \qquad (22)\end{aligned}$$

and

$$\begin{aligned}\hat{\mathbf{z}}_{\mathrm{UE}} &= \mathcal{F}^{\mathrm{Decry}}_{\mathrm{UE}}(\mathbf{y}'_{\mathrm{UE}}; \boldsymbol{\theta}^{\mathrm{Decry}}_{\mathrm{UE}}) \\ &= \underbrace{\mathbf{y}'_{\mathrm{UE}} - \mathcal{H}^{\mathrm{Decry}}_{\mathrm{UE}}(\mathbf{y}'_{\mathrm{UE}}; \bar{\boldsymbol{\theta}}^{\mathrm{Decry}}_{\mathrm{UE}})}_{\text{ARN at downlink UE}} \qquad (23) \\ &= \mathbf{y}'_{\mathrm{UE}} - \hat{\boldsymbol{o}}_{\mathrm{UE}}, \qquad (24)\end{aligned}$$

where $\mathcal{H}^{\mathrm{Decry}}_{\mathrm{BS}}(\cdot)$ and $\mathcal{H}^{\mathrm{Decry}}_{\mathrm{UE}}(\cdot)$ denote the DNN blocks at the ISAC BS and downlink UE, respectively. Their corresponding network parameters are $\bar{\boldsymbol{\theta}}^{\mathrm{Decry}}_{\mathrm{BS}}$ and $\bar{\boldsymbol{\theta}}^{\mathrm{Decry}}_{\mathrm{UE}}$, respectively. Here, $\hat{\boldsymbol{o}}_{\mathrm{BS}}$ and $\hat{\boldsymbol{o}}_{\mathrm{UE}}$ are the estimation results of $\boldsymbol{\delta}+\mathbf{n}_{\mathrm{BS}}$ and $\boldsymbol{\delta}+\mathbf{n}_{\mathrm{UE}}$ (i.e., sum of adversarial attack and noise), respectively.

According to (19), (21), and (23), the proposed SS-ISAC framework needs to jointly train $\mathcal{H}^{\mathrm{Encry}}(\cdot)$, $\mathcal{H}^{\mathrm{Decry}}_{\mathrm{BS}}(\cdot)$, and $\mathcal{H}^{\mathrm{Decry}}_{\mathrm{UE}}(\cdot)$ in the designed ARNs, with the corresponding network parameters set as $\bar{\boldsymbol{\Theta}}_{\mathrm{Security}} = \{\bar{\boldsymbol{\theta}}^{\mathrm{Encry}}, \bar{\boldsymbol{\theta}}^{\mathrm{Decry}}_{\mathrm{BS}}, \bar{\boldsymbol{\theta}}^{\mathrm{Decry}}_{\mathrm{UE}}\}$. In the following, the loss function, $\mathcal{L}(\bar{\boldsymbol{\Theta}}_{\mathrm{Security}})$, is precisely

devised for the ARN training. To pursue the tradeoff between SAC performance and ensure system security, $\mathcal{L}(\bar{\mathbf{\Theta}}_{\rm Security})$ is constructed by four parts: the first part $\mathcal{L}_{\rm pow}$ constrains the power of the adversarial attack $\boldsymbol{\delta}$, the second part $\mathcal{L}_{\rm sen}$ and third part $\mathcal{L}_{\rm com}$ respectively characterize the SAC performance at the legitimate ISAC BS and downlink UE, and the fourth part $\mathcal{L}_{\rm pri}$ describes the privacy information leakage risk to the eavesdropper Eve. As such, $\mathcal{L}(\bar{\mathbf{\Theta}}_{\rm Security})$ is formulated as

$$\begin{aligned}&\mathcal{L}(\bar{\mathbf{\Theta}}_{\rm Security})\\&\quad=\lambda_{\rm pow}\mathcal{L}_{\rm pow}+\lambda_{\rm sen}\mathcal{L}_{\rm sen}+\lambda_{\rm com}\mathcal{L}_{\rm com}+\lambda_{\rm pri}\mathcal{L}_{\rm pri},\end{aligned}\tag{25}$$

where $\lambda_{\rm pow}$, $\lambda_{\rm com}$, $\lambda_{\rm sen}$, and $\lambda_{\rm pri}$ are the hyperparameters used to pursue the tradeoff among multiple objectives. The loss function $\mathcal{L}_{\rm pow}$ is designed to limit the power of $\boldsymbol{\delta}$ as

$$\mathcal{L}_{\rm pow}=\max\Big(0,\frac{1}{L_{\rm t}}\|\boldsymbol{\delta}\|^2-\tau\Big).\tag{26}$$

Note that $\mathcal{L}_{\rm pow}$ aims to severely punish the deviations that exceed the power limit τ, while no punishment when $\boldsymbol{\delta}$ uses less power. The loss function $\mathcal{L}_{\rm sen}$ is devised to characterize the estimation accuracy of the target azimuth angle as

$$\mathcal{L}_{\rm sen}=\mathbb{E}\|\hat{x}_{\rm BS}-\phi\|^2.\tag{27}$$

The loss function $\mathcal{L}_{\rm com}$ describes the image data reconstruction performance as

$$\mathcal{L}_{\rm com}=\mathbb{E}\|\hat{\mathbf{x}}_{\rm UE}-\mathbf{x}\|^2.\tag{28}$$

Regarding (27) and (28), the MSE losses are employed since the considered SAC tasks are the target azimuth angle estimation and image transmission, respectively. It is worth mentioning that the proposed SS-ISAC framework can be flexibly extended to other SAC tasks by adjusting $\mathcal{L}_{\rm sen}$ and $\mathcal{L}_{\rm com}$, considering the practical SAC demands. As for Eve, consider the image label as its desired privacy information. The loss function $\mathcal{L}_{\rm pri}$ is designed as the confidence level of the image $\mathbf{x}$ being classified as the true image label $\mathbf{v}$. Then, $\mathcal{L}_{\rm pri}$ is given by

$$\mathcal{L}_{\rm pri}=\mathbb{E}\|r_k\|^2=\mathbb{E}\left\|\frac{e^{\beta_k}}{\sum_{k=1}^{K}e^{\beta_k}}\right\|^2,\tag{29}$$

where r_k denotes the confidence level obtained by the *Softmax* function, and K is the total number of the image categories. Here, the output β_k from the k-th neuron in the final layer of the Eve's classifier is used to describe the confidence level when $\mathbf{x}$ is correctly classified as $\mathbf{v}$. It can be implied from (29) that the higher the confidence level achieved, the greater the punishment suffered during network training. By utilizing the loss functions in (26)-(29), $\mathcal{L}(\bar{\mathbf{\Theta}}_{\rm Security})$ in (25) can be constructed. Finally, the optimal parameters set $\hat{\mathbf{\Theta}}_{\rm Security}=\{\hat{\boldsymbol{\theta}}^{\rm Encry},\hat{\boldsymbol{\theta}}^{\rm Decry}_{\rm BS},\hat{\boldsymbol{\theta}}^{\rm Decry}_{\rm UE}\}$ is obtained by minimizing $\mathcal{L}(\bar{\mathbf{\Theta}}_{\rm Security})$ as

$$\hat{\mathbf{\Theta}}_{\rm Security}=\underset{\bar{\mathbf{\Theta}}_{\rm Security}}{\arg\min}\,\mathcal{L}\big(\bar{\mathbf{\Theta}}_{\rm Security}\big).\tag{30}$$

The problem in (30) can be solved by using the stochastic gradient descent method. The training dataset is denoted by $\mathcal{S}=\{(\mathbf{x}_{(1)},\mathbf{v}_{(1)},\phi_{(1)}),(\mathbf{x}_{(2)},\mathbf{v}_{(2)},\phi_{(2)}),\quad\ldots,(\mathbf{x}_{(L)},\mathbf{v}_{(L)},\phi_{(L)})\}$, where $(\mathbf{x}_{(l)},\mathbf{v}_{(l)},\phi_{(l)})$ represents the l-th training sample and L is the size of $\mathcal{S}$. It should be noted that when training $\bar{\mathbf{\Theta}}_{\rm Security}$, the network parameters set $\hat{\mathbf{\Theta}}_{\rm General}$ of the original GS-ISAC system is frozen and does not need to be repeatedly trained. Hence, the distinct advantage of the proposed SS-ISAC framework is that only the paired pluggable modules need to be trained based on the security demands, instead of retraining the entire system. This significantly reduces the training cost. On the other hand, the designed ARN-based paired pluggable modules can be flexibly removed when there are no security demands, without affecting the SAC performance of the original GS-ISAC system.

IV. Simulation Results

This section quantitatively assesses the performance of the proposed SS-ISAC framework. In simulations, $M=16$, $\mathbb{E}(\|\mathbf{z}\|^2)=1$, $\tau=0.1$, $\lambda_{\rm pow}=0.1$, $\gamma_{\rm sen}=\lambda_{\rm sen}=0.5$, $\gamma_{\rm com}=\lambda_{\rm com}=0.1$, and $\lambda_{\rm pri}=0.01$ unless further specified. The sensing target is randomly located in $\phi\in[-20^\circ,20^\circ]$. The simulations are performed on the MNIST dataset, which contains numerous handwritten digit images with a grayscale of 28×28 [7]. Adopt $60,000$ images of the MINIST dataset for training, and the remaining $10,000$ images for testing. The SE, JSCE, JSCD, and SD are respectively modeled as the fully connected neuron networks with one hidden layer. The SE, JSCE, JSCD, SD at the ISAC BS (i.e., $\mathcal{E}^{\rm SE}(\cdot)$, $\mathcal{E}^{\rm JSCE}(\cdot)$, $\mathcal{D}^{\rm JSCD}_{\rm BS}(\cdot)$, and $\mathcal{D}^{\rm SD}_{\rm BS}(\cdot)$) respectively contain 64 hidden neurons, while the SE and JSCD at the downlink UE (i.e., $\mathcal{D}^{\rm JSCD}_{\rm UE}(\cdot)$ and $\mathcal{D}^{\rm SD}_{\rm UE}(\cdot)$) respectively consists of 16 hidden neurons. The SE input size and JSCE output size are respectively $28\times28=784$ and 23, and thus, the compression ratio of the semantic transmitter is $\frac{23}{784}\approx0.03$. As for the proposed ARN-based paired pluggable modules, their DNN blocks (i.e., $\mathcal{H}^{\rm Encry}(\cdot)$, $\mathcal{H}^{\rm Decry}_{\rm BS}(\cdot)$, and $\mathcal{H}^{\rm Decry}_{\rm UE}(\cdot)$) are modeled as the fully connected neuron networks with two hidden layers, respectively. The two hidden layers in $\mathcal{H}^{\rm Encry}(\cdot)$ and $\mathcal{H}^{\rm Decry}_{\rm BS}(\cdot)$ respectively contain 23 and 64 neurons, while those in $\mathcal{H}^{\rm Decry}_{\rm UE}(\cdot)$ respectively consist of 23 and 16 neurons. As for Eve, the adopted classifier $\mathcal{P}_{\rm Eve}(\cdot)$ is a fully connected neural network consisting of three hidden layers, with 64, 32, and 32 neurons in each layer, respectively. All the hidden layers adopt *ReLU* activation functions. The *Adam* optimizer is adopted to update the network parameters, with the learning rate of 10^{-4} and batch size of 256.

Fig. 3 evaluates the MSE performance of the SAC tasks and the correct classification probability P_c of the eavesdropper Eve under various SNR conditions. Consider SNR $=15\,\rm dB$ in the training procedure, while SNR $=[0,20]\,\rm dB$ with a step size of $5\,\rm dB$ for testing. The SNR used in the simulations refers to that at the receiver side. "White box" indicates that the proposed SS-ISAC framework has the prior knowledge of Eve's classifier $\mathcal{P}_{\rm Eve}$, allowing the ARN-based paired pluggable modules to be trained using the true model of $\mathcal{P}_{\rm Eve}$. On the contrary, "Black box" means that the proposed SS-ISAC lacks the prior knowledge of $\mathcal{P}_{\rm Eve}$. Then, a local substitute model of $\mathcal{P}_{\rm Eve}$, which is a fully connected neural network constructed by two hidden layers with 16 neurons each, is employed during

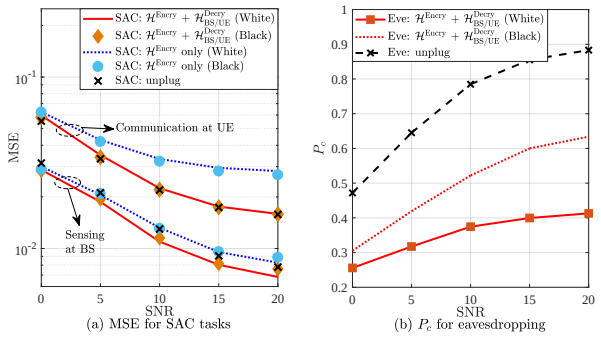

(a) MSE for SAC tasks (b) P_c for eavesdropping

Fig. 3. MSE and P_c performance versus SNR: (a) MSE for SAC tasks, (b) P_c for eavesdropping at Eve.

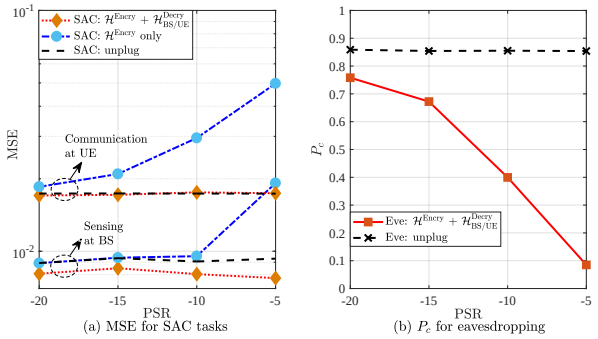

(a) MSE for SAC tasks (b) P_c for eavesdropping

Fig. 4. MSE and P_c performance versus PSR: (a) MSE for SAC tasks, (b) P_c for eavesdropping at Eve.

the ARN training. It can be noted that the local substitute model in the black box case is significantly different from the true model of $\mathcal{P}_{\text{Eve}}$ in the white box case. As shown in Fig. 3(a), the SAC tasks achieve superior MSE performance when simultaneously adopting the paired pluggable encryption and decryption modules (i.e., $\mathcal{H}^{\text{Encry}}(\cdot)$ and $\mathcal{H}^{\text{Decry}}_{\text{BS/UE}}(\cdot)$), compared to the case with $\mathcal{H}^{\text{Encry}}_{\text{BS/UE}}(\cdot)$ only. Moreover, compared to the SAC performance in the original GS-ISAC system without security consideration (i.e., "unplug" case), the proposed SS-ISAC framework with both $\mathcal{H}^{\text{Encry}}(\cdot)$ and $\mathcal{H}^{\text{Decry}}_{\text{BS/UE}}(\cdot)$ achieves better sensing MSE and comparable communication MSE. The above findings unveil that $\mathcal{H}^{\text{Encry}}(\cdot)$ and $\mathcal{H}^{\text{Decry}}_{\text{BS/UE}}(\cdot)$ respectively possess considerable encryption and decryption capacities. As observed from Fig. 3(b), P_c at Eve drops by around 50% under SNR $= 20\,\text{dB}$ after adopting $\mathcal{H}^{\text{Encry}}(\cdot)$ and $\mathcal{H}^{\text{Decry}}_{\text{BS/UE}}(\cdot)$, revealing the superior attack capacity of the proposed SS-ISAC framework. Moreover, one can observe that when comparing the white box and black box cases, the MSE for the SAC tasks is comparable, and P_c increases but within an acceptable range in the black box case. This essential observation relaxes the demand for prior knowledge of Eve.

Fig. 4 investigates the impact of the perturbation-to-signal ratio (PSR) on the MSE and P_c performance. Here, PSR represents the ratio between the adversarial perturbation power limit τ and transmit signal power $\mathbb{E}(\|\mathbf{z}\|^2)$. The SNR is fixed to $15\,\text{dB}$. One can note that even when PSR $= -20\,\text{dB}$ (i.e., τ is only 1% of $\mathbb{E}(\|\mathbf{z}\|^2)$), P_c at Eve can be reduced by around 10%, while the SAC tasks remain promising MSE performance after adopting $\mathcal{H}^{\text{Encry}}(\cdot)$ and $\mathcal{H}^{\text{Decry}}_{\text{BS/UE}}(\cdot)$. Moreover, P_c at Eve shows an apparent decreasing trend with the increase of PSR, and Eve's classifier is nearly invalid when PSR $= -5\,\text{dB}$. The above findings unveil the considerable SAC performance and superior attack capacity of the proposed SS-ISAC framework under various PSR conditions.

V. Conclusion

This paper has proposed a SS-ISAC framework equipped with the ARN-based paired pluggable encryption and decryption modules. The encryption module at the legitimate transmitter has been developed to generate the adversarial attack, while the decryption module at the legitimate receiver has been devised to mitigate the adversarial attack and noise. The above two modules have been jointly optimized, taking into account both the SAC requirements of the legitimate transceiver, as well as the privacy leakage risk to Eve. Numerical results have indicated that under different SNR conditions, the proposed SS-ISAC framework provides a considerable SAC performance and significantly reduces privacy leakage risk (e.g., P_c drops by around 50% at SNR $= 20\,\text{dB}$), compared to the case without encryption and decryption modules. Furthermore, the proposed SS-ISAC framework has been evaluated under various PSN conditions, revealing promising SAC performance and superior attack capacity.

References

[1] Z. Du, F. Liu, Y. Li, W. Yuan, Y. Cui, Z. Zhang, C. Masouros, and B. Ai, "Toward ISAC-empowered vehicular networks: Framework, advances, and opportunities," *IEEE Wireless Commun.*, vol. 32, no. 2, pp. 222–229, Apr. 2025.

[2] N. Su, F. Liu, and C. Masouros, "Sensing-assisted eavesdropper estimation: An ISAC breakthrough in physical layer security," *IEEE Trans. Wireless Commun.*, vol. 23, no. 4, pp. 3162–3174, Apr. 2024.

[3] Y. Liu, I. Al-Nahhal, O. A. Dobre, and F. Wang, "Deep-learning channel estimation for IRS-assisted integrated sensing and communication system," *IEEE Trans. Veh. Technol.*, vol. 72, no. 5, pp. 6181–6193, May 2023.

[4] W. Ding, Z. Yang, M. Chen, Y. Liu, and M. Shikh-Bahaei, "Joint vehicle connection and beamforming optimiziation in digital-twin-assisted integrated sensing and communication vehicular networks," *IEEE Internet Things J.*, vol. 11, no. 20, pp. 32 923–32 938, Oct. 2024.

[5] X. Meng, F. Liu, C. Masouros, W. Yuan, Q. Zhang, and Z. Feng, "Vehicular connectivity on complex trajectories: Roadway-geometry aware ISAC beam-tracking," *IEEE Trans. Wireless Commun.*, vol. 22, no. 11, pp. 7408–7423, Nov. 2023.

[6] W. Yuan, F. Liu, C. Masouros, J. Yuan, D. W. K. Ng, and N. Gonzlez-Prelcic, "Bayesian predictive beamforming for vehicular networks: A low-overhead joint radar-communication approach," *IEEE Trans. Wireless Commun.*, vol. 20, no. 3, pp. 1442–1456, Mar. 2021.

[7] B. He, F. Wang, and T. Q. S. Quek, "Secure semantic communication via paired adversarial residual networks," *IEEE Wireless Commun. Lett.*, vol. 13, no. 10, pp. 2832–2836, Oct. 2024.

[8] N. Wu, R. Jiang, X. Wang, L. Yang, K. Zhang, W. Yi, and A. Nallanathan, "AI-enhanced integrated sensing and communications: Advancements, challenges, and prospects," *IEEE Commun. Mag.*, vol. 62, no. 9, pp. 144–150, Sep. 2024.

[9] J. Dai, H. Fan, Z. Zhao, Y. Sun, and Z. Yang, "Secure resource allocation for integrated sensing and semantic communication system," in *Proc. ICC Workshops*, Aug. 2024, pp. 1225–1230.

[10] Y. Yang, Z. Yang, W. Yuan, F. Liu, X. Cao, C. Huang, Z. Zhang, and M. Shikh-Bahaei, "Integrated sensing, computing and secure semantic communication for smart healthcare systems," in *Proc. GC Workshops*, Dec. 2024, pp. 1–6.

[11] A. Faisal, I. Al-Nahhal, O. A. Dobre, and T. M. N. Ngatched, "Deep reinforcement learning for optimizing RIS-assisted HD-FD wireless systems," *IEEE Commun. Lett.*, vol. 25, no. 12, pp. 3893–3897, Dec. 2021.